

X-RAY EMISSION OF STARBURST GALAXIES

Gerhard Hensler¹, Ralph Dickow¹, and Norbert Junkes²

RESUMEN

Presentamos observaciones hechas con *ROSAT*, PSPC y HRI, de cuatro galaxias enanas con brotes de formación estelar: He 2-10, Mrk 297, III Zw 102, and NGC 1705. Damos una descripción de los espectros en rayos X y de las diferencias encontradas. También damos una breve descripción de nuestras interpretaciones. Para dos casos (He 2-10 y Mrk 297), la emisión puede ser entendida por aumentos en algunas abundancias de elementos debidas a supernovas de tipo II. El espectro de III Zw 102 es plano, mientras que el de NGC 1705 tiene sólo rayos X suaves, sin la emisión característica de los brotes arriba de 1 keV.

ABSTRACT

We present results from *ROSAT*, PSPC and HRI observations of four starburst dwarf galaxies: He 2-10, Mrk 297, III Zw 102, and NGC 1705. This paper provides the documentation of their X-ray spectra, and describes some of their differences. We also give a brief discussion of the interpretations. For two spectra (He 2-10 and Mrk 297), the fit can be significantly improved taking particular element enhancements of supernova type II yields into account instead of considering a Raymond-Smith spectrum with purely solar abundances. The spectrum of III Zw 102 reveals a flat distribution, while NGC 1705 is showing an extreme exception by only a very soft X-ray part but without the characteristic emission of starbursts above 1 keV.

Key words: GALAXIES: COMPACT — GALAXIES: STARBURST — X-RAYS: GALAXIES

1. INTRODUCTION

Low-mass galaxies fall into a regime in the parameter space where they should behave like disks of spiral galaxies, namely, their star-formation should be strictly self-regulated (Köppen et al. 1995) because the energy release of massive stars greatly exceeds the gravitational energy of the interstellar medium (ISM). From dynamical models of dwarf galaxies (Hensler et al. 1993, 1996d), however, their evolution could be strongly influenced by stochastic epochs of intense star formation which can originate intrinsically by a gas recollapse, but can also be caused by dynamical effects like gas infall (e.g., He 2-10) or external perturbations (see Brinks, this volume). This allows only a few generations of stars to form during the lifetime of such a galaxy. Many dwarf galaxies contain mainly older stellar populations but have sufficient amounts of ISM to expire an episode of relatively high star-formation activity. Such objects appear as starburst galaxies because their current star-formation rate (SFR) greatly exceeds the time-averaged one. Surprisingly, this starburst phenomenon is often locally confined to massive star clusters (super starclusters: SSC), like e.g., the two SSCs in He 2-10 (Vacca & Conti 1992) and in NGC 1569 (O’Connell et al. 1994), and the single central SSC in NGC 1705, which are supposed to represent the same stellar “building blocks” with the same star-formation vehemence like proto-Globular Clusters at earlier epochs (see Ho, this volume) or also nowadays in merging galaxies. Therefore, studies of nearby starburst dwarf galaxies (SBDGs) present an outstanding opportunity to improve our insight into the structure of the star-forming sites and the star-forming process itself. SBDGs are characterized by huge H_α regions that go far beyond the sizes of the star-forming regions. Moreover, the H_α contours are structured and appear as plumes, filaments, arcs or loops, which are expanding. Because accumulated supernovae type II (SNe II) explosions within the SSCs form a huge hot gas plumes which expand and sweep up surrounding gas spatially high-resolved X-ray observations of SBDGs often discover a clear connection of X-ray maxima with the

¹Institut für Astronomie und Astrophysik, Universität Kiel, Olshausenstr. 40, D-24098 Kiel, Germany, e-mail: hensler@astrophysik.uni-kiel.de.

²Astrophysikalisches Institut Potsdam, An der Sternwarte 16, D-14482 Potsdam, Germany.

SSCs (e.g., in NGC 1569, Heckman et al. 1995, or in He 2-10, see below) or are enveloped by the H_α loops like in NGC 4449 (Bomans et al. 1996) or in NGC 1705 (see below). In this paper we wish to present our *ROSAT* observations of four starburst galaxies with particular emphasis on the spectra taken with the Position Sensitive Proportional Counter (PSPC). For this we firstly introduce possible spectral models which are applicable to starburst observations and discuss, in the following sections, the implications of the different spectral models when fitted to the PSPC data of different SBDGs. In addition, high spatial-resolution exposures have been taken using the High Resolution Imager (HRI). Because of the paper-size limitation we can only draw the readers' attention to some emerging problems and refer to ongoing work in more comprehensive publications.

2. SPECTRAL MODELS

There are two different basic models of X-ray spectra in the *ROSAT* band concerning those extragalactic sources of investigation which are caused by their different origin:

2.1. Power Law

A power law spectrum $E^{-\alpha}dE$ with the spectral index α is attributed to the X-ray emission of active galactic nuclei (AGN) and of high-mass X-ray binaries (HMXRB) in SBDGs. These sources have spectra consisting of two components: the high-energy part at energy $E > 2$ keV can be fitted by a power law with an index $\alpha \approx 1.7$ for AGNs and $\alpha = 0.8 - 1.5$ for HMXRBs (Nagase 1989); at $0.1 \text{ keV} < E < 2 \text{ keV}$ – i.e., almost within the *ROSAT* band – steeper power-law indices of $\alpha = 2.4$ for AGNs and of $\alpha \approx 2.7$ for HMXRBs are called the “soft excess” (Mavromataki 1993). Since both sources are also typically representing galactic activity, their spectral contributions must be studied and can often not be neglected. We denote the power-law model as POWER.

2.2. Raymond-Smith Model

In addition to a bremsstrahlung continuum radiation of a hot, tenuous plasma the recombination continuum and emission of both recombination and collisionally excited spectral lines contribute significantly to the spectra and depend on the abundances of heavy elements and the temperature. This emission is usually modelled using the code by Raymond & Smith (1977) and applied to interpret the X-ray spectra of superbubbles in starburst regions. The emission is also absorbed by gas in our Galaxy, in the observed object itself and by intergalactic gas. This absorption is considered in all the model spectra and depends on the equivalent column density of hydrogen N_H (Morrison & McCammon 1983). This value can be compared with column densities $N_{H,gal}$ from H I observations at 21 cm of the Galaxy in the direction of the target (Dickey & Lockman 1990).

2.3. The Effect of Element Abundances on the Raymond-Smith Model

Usually, cosmic element abundances (Anders & Grevesse 1989) are considered in the Raymond-Smith model and we denote those furtheron as RAYMOND. Nonetheless, the hot plasma in superbubbles should contain nucleosynthesis products of the SNe II progenitors in excess and presumably of the explosions themselves. There is a lack of knowledge and expertise because of the complexity of its modelisation as to what amount specific elements are enhanced or reduced by means of explosive burning in SNe II. Therefore, as a first-order approximation and as the other extreme assumption in contrast to cosmic abundances we applied the integrated element abundances of massive stars for a Salpeter stellar mass distribution (IMF) from their hydrostatic burning under the assumptions of instantaneous release in the superbubbles and their non-mixing with the ambient medium. As a conservative way, here we apply results of the nucleosynthesis in massive stars by Woosley & Weaver (1986), integrate for $10-100 M_\odot$ and denote this model as W&W. Since the iron yield depends on the remnant mass and cannot be determined from stellar evolution models, we use an approximation by Matteucci (1986) which is consistent with determinations of the Fe mass in the supernova 1987a. For more details we refer to Dickow et al. (1996). Since the spectral resolution of the PSPC detector needs large changes of element abundances in the Raymond-Smith spectrum in order to alter the binned X-ray counts significantly, on the other hand, it is impossible to determine single abundance values from model fits to observed spectra. Therefore, *ROSAT* spectra cannot provide sufficient information to allow for precise abundance determinations, but to reveal large anomalies qualitatively. With respect to RAYMOND and W&W the X-ray spectra of a sample of SBDGs show larger count rates at energies slightly above 1.3 keV (Dickow 1995). Since in this energy range the line emission could be mainly produced by magnesium and in order to get a first insight as to what amount

TABLE 1
ELEMENT ABUNDANCES AND METALLICITY FOR THE RAYMOND-SMITH
MODELS (SEE TEXT) RELATIVE TO THE COSMIC ABUNDANCES
FROM ANDERS & GREVESSE

Element	He	C	N	O	Ne	Mg	Si	S	Ar	Ca	Fe	Ni	Z
W&W (W&WMg)	1.7	4.2	3.8	17.4	8.5	8.8 (50)	44	52	47	62	7.6	7.6	13 (15)

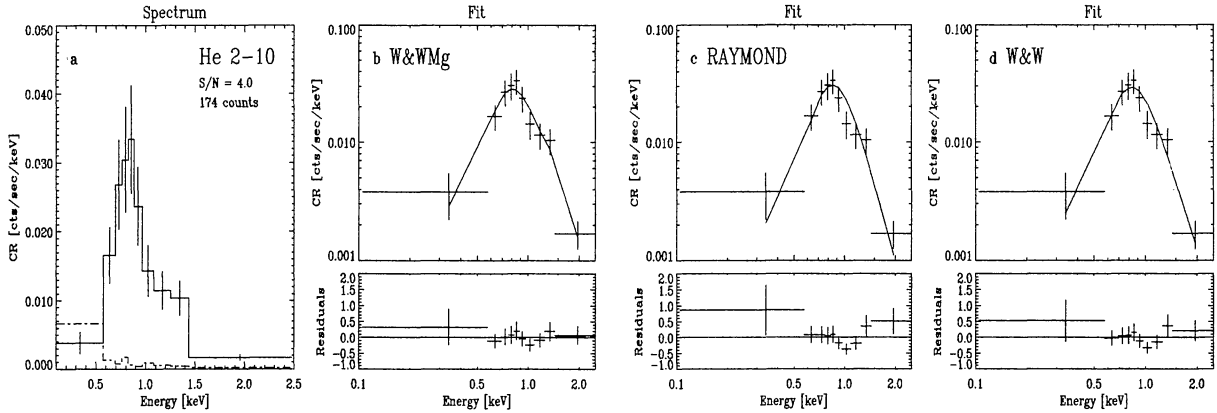


Fig. 1. *a*) X-ray spectrum of He 2-10 with background-(dash-dotted) taken with the *ROSAT* PSPC: count rates (CR) over energy. *b-d*) Fits of the models W&WMg, RAYMOND and W&W with relative residuals in the lower panels.

particular abundance changes affect the model spectrum, as a second-order effect we raise the magnesium abundance of W&W arbitrarily by a factor of almost 5.5 and denote this as model W&WMg (Table 1). The artificial enhancement of Mg in our W&W abundances also increases the total metal content to 15 times the cosmic one. That model W&WMg can partly achieve a better spectral fit will be demonstrated in the next for two objects, He 2-10 and Mrk 297, but it is also valid e.g., for the halo of M82 (Dickow et al. 1996).

3. HE 2-10

The dwarf galaxy He 2-10 (ESO 495-G21 and PK248+08) shows a compact appearance and blue colors, has a high gas content and low metallicity. Therefore, it is a typical example of a blue compact dwarf galaxy with enhanced star formation of numerous young massive stars in a starburst. Two SSCs are visible in the galaxy aligned in east-west direction and separated by $8''$ which amounts to 350 pc at a distance of 9 Mpc. For the brighter region SSC A in the west the number of Wolf-Rayet stars has been estimated to amount to 300–400 while the number of hot O-type stars reaches several ten thousands (Vacca & Conti 1992). *HST* images with the Faint Object Camera (Conti & Vacca 1994) in addition detected the division of SSC A into nine smaller subunits with diameters of only approximately 10 pc. Recent CO and H I observations of He 2-10 by Kobulnicky et al. (1995) discovered a large and thick H I disk extending over the whole V-band galactic body and an elongated CO structure embedded in the H I disk and with the same orientation. The *ROSAT* HRI contours in Fig. 4. (Plate 1), show one strong absolute maximum, which strikingly coincides with SSC A, and a local maximum to the east close to but not coinciding with the SSC B and inclined towards the elongated CO tail at SE. The X-ray spectrum of SSC A has been studied by us and is compared with different spectral fit models. From Fig. 1, one already recognizes clearly the enhanced emission below 1.5 keV. Accordingly the W&WMg model fits superior. However, the consequences for the parameter determination are drastical. While the N_{H} varies only by a factor of 2, for the X-ray luminosity a deviation between RAYMOND and W&WMg by one order of magnitude results, and the same for n_e (see Table 2).

TABLE 2

FIT PARAMETERS FOR THE SPECTRUM OF HE 2-10 WITH 1σ ERRORS. (THE NUMBER OF DEGREES OF FREEDOM IS $\nu = 7$)

Model	χ^2/ν	N_H [10^{21}cm^{-2}]	kT [keV]	F_X [$\text{erg cm}^{-2} \text{s}^{-1}$]	L_X [erg s^{-1}]	n_e [cm^{-3}]
POWER	1.0	5.4 ± 2.7	$\alpha = 5.9 \pm 1.7$	$(1.4^{+28}_{-1.3}) \cdot 10^{-9}$	$(1.4^{+27}_{-1.3}) \cdot 10^{43}$	
RAYMOND	1.7	$9.3^{+1.2}_{-2.2}$	$0.20^{+0.12}_{-0.02}$	$(2.1 \pm 0.1) \cdot 10^{-11}$	$(2.0 \pm 0.1) \cdot 10^{41}$	$8.4^{+3.5}_{-5.0}$
W&W	1.0	7.8 ± 1.7	$0.24^{+0.09}_{-0.05}$	$(1.0 \pm 0.2) \cdot 10^{-11}$	$(9.7 \pm 1.9) \cdot 10^{40}$	$1.5^{+1.3}_{-0.6}$
W&WMg	0.5	4.8 ± 2.9	$0.31^{+0.17}_{-0.09}$	$(1.8^{+0.5}_{-0.1}) \cdot 10^{-12}$	$(1.7^{+0.5}_{-0.1}) \cdot 10^{40}$	$0.68^{+0.95}_{-0.32}$

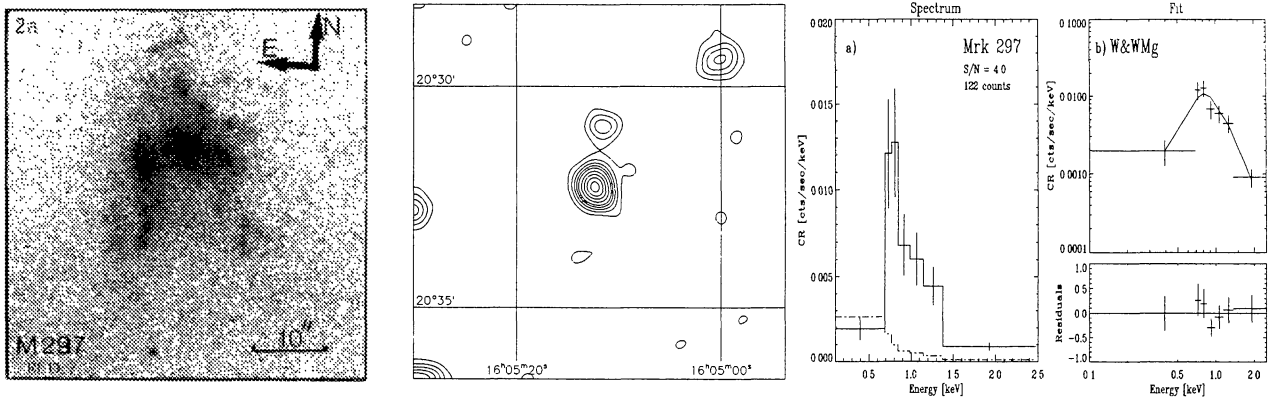


Fig. 2. a) Red image of Mrk 297; middle: *ROSAT* PSPC contours of Mrk 297. The contours have been convolved with a gauss function of $20''$ FWHM. The X-ray background is $(1.0 \pm 0.4) \cdot 10^{-3} \text{ cts arcmin}^{-2} \text{ s}^{-1}$; the contours are $3, 6, 9, 12, 15, 20, 25, 30, 35 \cdot \sigma$; right: a. X-ray spectrum of Mrk 297 with background (dash-dotted) taken with the *ROSAT* PSPC : count rates (CR) over energy. b) Fit of the model W&WMg with relative residuals in the lower panel.

4. MRK 297

Although Mrk 297 (NGC 6052, Arp 209) is visible at a distance of 64 Mpc and cannot entirely be spatially resolved in X-rays, its optically discernible knots (Hecquet et al. 1987) origin from super-giant H II regions and thus reflect the starburst activity of this object. With almost something more than $10^{10} M_{\odot}$ Mrk 297 belongs to the high-mass end of SBDGs. The X-ray PSPC contours (Fig. 2) are well concentric around the optical galactic body, while the HRI contours (not presented here, because still in progress) show a broad maximum with an extended halo. The spectrum contains the same indications of deviations from a RAYMOND model and also is strikingly much better fitted by W&WMg like He 2-10. The X-ray luminosity could only be determined with large uncertainty to almost $2 \cdot 10^{41} \text{ erg/s}$. For more details see a comprehensive paper (Hensler et al. 1996c) where the issues of our analysis will be published.

5. III ZW 102

Also III Zw 102 (NGC 7625, Arp 212) at a distance of 23 kpc with $3 \cdot 10^{10} M_{\odot}$ belongs to the very massive end of the SBDGs where one can doubt whether it could really be denoted "dwarf galaxy". III Zw 102 consists of a complex H_{α} structure and was observed by us with the *ROSAT* PSPC. Considering the X-ray spectrum (Fig. 3), it is noticeable that in contrast to the objects presented before between 0.6 and 1.3 keV a plateau exists. This causes a kind of neutrality for comparison with model spectra which fit all to quite the same quality (so that we avoid to present them here). Nevertheless, it should be mentioned that even in this case the W&WMg model yields a gradually better agreement with the binned observations. The X-ray luminosity amounts to $1.6 \cdot 10^{40} \text{ erg/s}$.

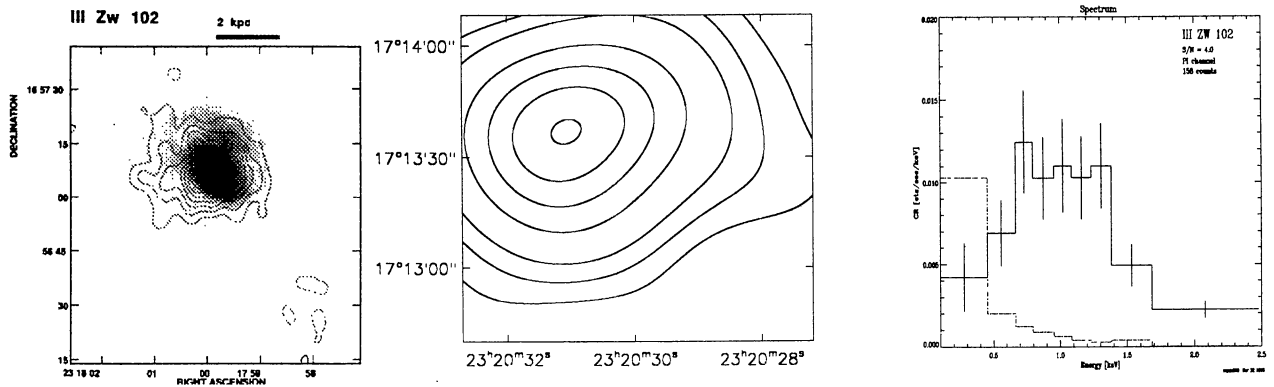


Fig. 3. *a)* Overlay of radio contours at $\nu = 1.489$ GHz with a B-band image of III Zw 102 (Deeg et al. 1993) (coordinates' epoch at 1950.0); middle: *ROSAT* PSPC contours of III Zw 102. The contours have been convolved with a gauss function of $20''$ FWHM. The X-ray background is $(1.1 \pm 0.4) \cdot 10^{-3}$ cts arcmin $^{-2}$ s $^{-1}$; the contours are 3, 6, 10, 20, 30, 40, 50 $\cdot \sigma$ (coordinates' epoch at 2000.0). Both figures represent almost the same section. *b)* X-ray spectrum of III Zw 102 taken with the *ROSAT* PSPC.

6. NGC 1705

NGC 1705 is a nearby very low-mass irregular galaxy ($1.2 \cdot 10^8 M_{\odot}$, Meurer et al. 1992) at a distance of 5 Mpc which shows striking signatures in H_{α} of a presently strong star-formation activity. It consists of one young SSC in the nucleus (O'Connell et al. 1994) with an age of about 10 Myrs and two older populations (Meurer et al. 1992). The H_{α} image (Fig. 5, Plate 2) of NGC 1705 shows loops and arcs that are strikingly accounting for expulsive events. Split emission lines with typical radial velocity differences of about 100 km s^{-1} agree with the model of outflowing gas that is expelled from the starbursting nucleus since 10^7 yrs. O'Connell et al. found that the total brightness and surface brightness within the half-light radius for this SSC fit on average to those values of the two NGC 1569 clusters but exceed the LMC star-forming region R136 by a factor 5 to 8, respectively. It is evident to expect that SNe II explosions from the SSC could produce a hot gas phase which cannot be kept bound by the low potential energy but has to be expelled from the galaxy. Two X-ray maxima east and west can be attributed to the main body of NGC 1705. Since they are fitting almost perfectly into the H_{α} holes surrounded by the loops (see Fig. 5, Plate 2), they obtrude convincingly the picture of hot X-ray bubbles surrounded by shells. A comparison with the H I disk of NGC 1705 (Meurer 1993) even shows that the line connecting both maxima is oriented perpendicularly to the disk direction. The blobs have distances of about $30''$ (0.7 kpc) from the center. Because of this symmetry and the existence of only one central star cluster one can assume that we are dealing with only one single hot superbubble produced by accumulated SNe II explosions. The main body of that bubble is still sticking in the disk and therefore hidden in X-rays, while the two sources represent those parts of highest expansion from the disk plane. The X-ray spectra of both sources are similar but abnormally soft. The sum of both is shown in Fig. 5 (Plate 2). In contrast to similar SBDGs like e.g., NGC 1569 (Heckman et al. 1995), NGC 4449 (Bomans et al. 1996, Dickow 1995), or NGC 5253 (Martin & Kennicutt 1995; Dickow 1995), which are still bright between 0.7–1.0 keV and possess maxima there corresponding to the PSPC sensitivity, the spectrum of NGC 1705 has its maximum at 0.2 keV and declines steeply to higher energies, approaching zero already before 0.9 keV. Only NGC 4449 exhibits also a (second) maximum between 0.2–0.3 keV and contains at least one soft source (Bomans et al. 1996). This fact is a mysterious puzzle because even if there exists only a small amount of intrinsic N_{H} in NGC 1705, the galactic foreground absorption of $N_{\text{H,gal}} = 3.5 \cdot 10^{20} \text{ cm}^{-2}$ according to Dickey & Lockman (1990) would provide only a poor fit for a Raymond-Smith spectrum with such softness. The X-ray luminosity is determined to $1.26 \cdot 10^{38}$ erg/s only, and these observations will be further discussed elsewhere (Hensler et al. 1996b).

7. SUMMARY

We have presented different kinds of *ROSAT* PSPC spectra of SBDGs and demonstrated some interesting implications to fit these spectra and to understand the models. Although we cannot enter into a detailed discussion and evaluation of the parameters here, we wish to give hints for further work and refer to publications

in progress. One of the main issues which we wish to emphasize is the interpretation of the spectrum of He 2-10 and Mrk 297 by a thermal plasma with an abundance enhancement, here fiducially by one particular element. Since the spectral resolution of the *ROSAT* PSPC does not provide detailed spectral information in order to determine element abundances, significant deviations from a thermal plasma with solar abundances seem intruding. However, we also warn to overinterpret this conclusion. One could imagine that the low particle density of the hot X-ray gas has caused the recombination timescale to surpass the characteristic dynamical timescale. This leads to frozen-in ionisation stages and let the recombination lag behind the electron temperature. This so-called non-equilibrium ionisation has been invoked by Breitschwerdt & Schmutzler (1994) for an explanation of the discrepancies between ionized species and observed soft X-ray background of the local bubble. Therefore, deviations of observed spectra from fit models have to be investigated with sufficient care before quantitative conclusions become reliable.

This project has been supported by the Deutsche Agentur für Raumfahrtangelegenheiten (DARA) GmbH under grant No. 50 OR 9302 4 (NJ, RD).

REFERENCES

- Anders, E., & Grevesse, N. 1989, *Geochimica et Cosmochimica Acta* 53, 197
 Aufderheide, M. B., Baron, E., & Thielemann, F. K. 1991, *ApJ*, 370, 630
 Bomans, D., Chu, Y.-H., & Hopp, U. 1996, *ApJ*, submitted
 Breitschwerdt, D., & Schmutzler, T. 1994, *Nature*, 371, 774
 Conti, P. S., & Vacca, W. D. 1994, *ApJ*, 423, L97
 Deeg, H. J., et al. 1993, *ApJ*, 410, 626
 Dickey, J. M., & Lockman, F. J. 1990, *ARA&A*, 28, 215
 Dickow, R. 1995, Diploma thesis, University of Kiel
 Dickow, R., Hensler, G., & Junkes, N. 1995, *Proc. 11th IAP Meeting*, ed. D. Kunth et al., (Editions Frontières), 583
 _____ . 1996, *A&A*, submitted
 Heckman, T. M., et al. 1995, *ApJ*, 448, 98
 Hensler, G., Theis, C., & Burkert, A. 1993, *Proc. 3rd DAEC Meeting, The Feedback of Chemical Evolution on the Stellar Content in Galaxies*, ed. D. Alloin & G. Stasinska, 229
 Hensler, G., Dickow, R., Junkes, N., & Gallagher, J. S. 1996a, *Proc. of the International X-ray Conference, Röntgenstrahlung from the Universe*, ed. H. U. Zimmermann et al., MPE Report No. 263, 379
 _____ . 1996b, *ApJ*, submitted
 Hensler, G.; Dickow, R., & Junkes, N. 1997, *A&A*, in preparation
 Hensler, G., Theis, C., & Gallagher, J. S. 1996c, *A&A*, submitted
 Hequet, J., Coupinot, G., & Maucherat, A. J. 1987, *A&A*, 183, 13
 Hutsemekers, D., & Surdej, J. 1984, *A&A*, 133, 209
 Kobulnicky, H. A., et al. 1995, *AJ*, 110, 116
 Köppen, J., Theis, C., & Hensler, G. 1995, *A&A*, 296, 99
 Martin, C. L., & Kennicutt, R. C. 1995, *ApJ*, 447, 171
 Matteucci, F. 1986, *ApJ*, 305, L81
 Mavromatakis, F. 1993, *A&A*, 273, 147
 Meurer, G. R., Freeman, K. C., Dopita, M. A., & Cacciari, C. 1992, *AJ*, 103, 60
 Meurer, G. R. 1993, in *Proc. ESO/OHP Workshop*
 Morrison, R., & McCammon, D. 1983, *ApJ*, 270, 119
 Nagase, F. 1989, *PASJ*, 41, 1
 O'Connell, R. W., Gallagher, J. S., & Hunter, D. A. 1994, *ApJ*, 433, 65
 Raymond, J. C., & Smith, B. W. 1977, *ApJS*, 35, 419
 Vacca, W. D., & Conti, P. S. 1992, *ApJ*, 401, 533
 Woosley, S. E., & Weaver, T. A. 1986, in *IAU Coll. 89*, ed. D. Mihalas & K.H. Winkler, 91